

Supplementary Materials for Nonlinear Heisenberg Limit via Uncertainty Principle in Quantum Metrology

Binke Xia,^{1,2} Jingzheng Huang,^{1,3,4,*} Yuxiang Yang,^{2,†} and Guihua Zeng^{1,3,4,‡}

¹*State Key Laboratory of Advanced Optical Communication Systems and Networks,
Institute for Quantum Sensing and Information Processing,*

School of Sensing Science and Engineering, Shanghai Jiao Tong University, Shanghai 200240, China

²*QICI Quantum Information and Computation Initiative, School of Computing and Data Science,
The University of Hong Kong, Pokfulam Road, Hong Kong, China*

³*Hefei National Laboratory, Hefei 230088, China*

⁴*Shanghai Research Center for Quantum Sciences, Shanghai 201315, China*

* jzhuang1983@sjtu.edu.cn

† yxyang@hku.hk

‡ ghzeng@sjtu.edu.cn

Supplementary Note 1: Calculating the ultimate precision limits

In this section, we will give the details of calculating the ultimate precision limits in Eq. (2), Eq. (4), Eq. (5), and Eq. (7) of the main text. First, we investigate the ultimate precision limit in the standard quantum metrological scheme with a unitary parameterizing process $\hat{U}_S(g)$. Then the canonical momentum operator in the Heisenberg picture can be expressed as

$$\hat{\mathcal{K}}_S = \hat{U}_S^\dagger(g) \hat{K}_S \hat{U}_S(g) = i \hat{U}_S^\dagger(g) [\partial_g \hat{U}_S(g)] = \int_0^{T_S} \hat{U}_S^\dagger(0 \rightarrow t) [\partial_g \hat{H}_S(g)] \hat{U}_S(0 \rightarrow t) dt,$$

where $\hat{H}_S(g)$ is the Hamiltonian and T_S is the total evolution time of the parameterizing process. We denote $\hat{V}_S = \partial_g \hat{H}_S(g)$ as the characteristic operator of this dynamical process. Given that we only concern about the metrological scenarios with time-independent Hamiltonians, the above momentum operator can be rewritten as

$$\hat{\mathcal{K}}_S = \int_0^{T_S} e^{i\hat{H}_S t} \hat{V}_S e^{-i\hat{H}_S t} dt.$$

For a probe state $\hat{\rho}_S$ with the spectral decomposition $\hat{\rho}_S = \sum_i p_i |\psi_i\rangle\langle\psi_i|$, we can calculate its average uncertainty with respect to the canonical momentum operator $\hat{\mathcal{K}}_S$ as

$$\Delta\bar{\mathcal{K}}_S^2 = \sum_i p_i \left(\langle\psi_i|\hat{\mathcal{K}}_S^2|\psi_i\rangle - \langle\psi_i|\hat{\mathcal{K}}_S|\psi_i\rangle^2 \right) = \sum_i p_i \Delta_i \mathcal{K}_S^2,$$

where $\Delta_i \mathcal{K}_S = \sqrt{\langle\psi_i|\hat{\mathcal{K}}_S^2|\psi_i\rangle - \langle\psi_i|\hat{\mathcal{K}}_S|\psi_i\rangle^2}$ denotes the uncertainty of the i -the eigenstate $|\psi_i\rangle$ with respect to the canonical momentum operator $\hat{\mathcal{K}}_S$. Subsequently, we can calculate

$$\begin{aligned} \Delta_i \mathcal{K}_S^2 &= \langle\psi_i| \left(\int_0^{T_S} e^{i\hat{H}_S t} \hat{V}_S e^{-i\hat{H}_S t} dt \right)^2 |\psi_i\rangle - \left(\langle\psi_i| \int_0^{T_S} e^{i\hat{H}_S t} \hat{V}_S e^{-i\hat{H}_S t} dt |\psi_i\rangle \right)^2 \\ &= \int_0^{T_S} \langle\psi_i| e^{i\hat{H}_S t} \hat{V}_S e^{-i\hat{H}_S t} dt \cdot (\hat{\mathbb{I}} - |\psi_i\rangle\langle\psi_i|) \cdot \int_0^{T_S} e^{i\hat{H}_S t} \hat{V}_S e^{-i\hat{H}_S t} |\psi_i\rangle dt \\ &= \int_0^{T_S} \langle\psi_i| e^{i\hat{H}_S t} \hat{V}_S e^{-i\hat{H}_S t} (\hat{\mathbb{I}} - |\psi_i\rangle\langle\psi_i|) dt \cdot \int_0^{T_S} (\hat{\mathbb{I}} - |\psi_i\rangle\langle\psi_i|) e^{i\hat{H}_S t} \hat{V}_S e^{-i\hat{H}_S t} |\psi_i\rangle dt. \end{aligned}$$

Drawing on the Cauchy–Schwarz inequality of $|\int_a^b f(x)dx|^2 \leq (b-a) \int_a^b |f(x)|^2 dx$, we can derive

$$\begin{aligned} \Delta_i \mathcal{K}_S^2 &\leq T_S \int_0^{T_S} \langle\psi_i| e^{i\hat{H}_S t} \hat{V}_S e^{-i\hat{H}_S t} (\hat{\mathbb{I}} - |\psi_i\rangle\langle\psi_i|) e^{i\hat{H}_S t} \hat{V}_S e^{-i\hat{H}_S t} |\psi_i\rangle dt \\ &= T_S \int_0^{T_S} \left(\langle\psi_i| e^{i\hat{H}_S t} \hat{V}_S^2 e^{-i\hat{H}_S t} |\psi_i\rangle - \langle\psi_i| e^{i\hat{H}_S t} \hat{V}_S e^{-i\hat{H}_S t} |\psi_i\rangle^2 \right) dt. \end{aligned}$$

Then we can derive

$$\begin{aligned} \Delta\bar{\mathcal{K}}_S^2 &= \sum_i p_i \Delta_i \mathcal{K}_S^2 \\ &= T_S \int_0^{T_S} \sum_i p_i \left(\langle\psi_i| e^{i\hat{H}_S t} \hat{V}_S^2 e^{-i\hat{H}_S t} |\psi_i\rangle - \langle\psi_i| e^{i\hat{H}_S t} \hat{V}_S e^{-i\hat{H}_S t} |\psi_i\rangle^2 \right) dt \\ &= T_S \int_0^{T_S} \Delta\bar{V}_S^2|_{\hat{\rho}_t} dt, \end{aligned}$$

where $\hat{\rho}_t = \sum_i p_i e^{-i\hat{H}_S t} |\psi_i\rangle\langle\psi_i| e^{i\hat{H}_S t}$. Since the average uncertainty of the operator \hat{V}_S is bounded by a maximum value of $\Delta\mathcal{V}_S$, i.e., $\Delta\bar{V}_S^2 \leq \Delta\mathcal{V}_S^2$ for any quantum state in the Hilbert space with respect to the probe. Then we can determine that the uncertainty of the canonical momentum is bounded by

$$\Delta\bar{\mathcal{K}}_S^2 \leq \Delta\mathcal{V}_S^2 T_S^2 \Rightarrow \Delta\mathcal{K}_S \leq \Delta\mathcal{V}_S T_S. \quad (S1)$$

By assigning $T_S = T$ and substituting Eq. (S1) into Eq. (1), we can ultimately derive the precision limit as shown in Eq. (2).

Subsequently, we investigate the ultimate precision limit in our quantum metrological scheme with an ITD generating process $\hat{U}_I = \hat{U}_C \otimes |0\rangle\langle 0| + \hat{U}_C^\dagger \otimes |1\rangle\langle 1|$, where $|0\rangle$ and $|1\rangle$ are the complete orthogonal basis of the ancilla we employed for implementing the quantum switch. Here the unitary operator $\hat{U}_C = \exp(-i\hat{H}_C T_C)$ represents the evolution the generation process with the forward time direction, where \hat{H}_C is the Hamiltonian and T_C is the evolution time of this process. Given that the entire evolution in our scheme is written as $\hat{U}_{IS} = \hat{U}_S \hat{U}_C \otimes |0\rangle\langle 0| + \hat{U}_S \hat{U}_C^\dagger \otimes |1\rangle\langle 1|$, the canonical momentum operator in the parameter space of the joint system of probe and ancilla (in the Heisenberg picture) can be given by

$$\hat{\mathcal{K}}_I = i\hat{U}_{IS}^\dagger(g)[\partial_g \hat{U}_{IS}(g)] = \hat{U}_C^\dagger \hat{\mathcal{K}}_S \hat{U}_C \otimes |0\rangle\langle 0| + \hat{U}_C \hat{\mathcal{K}}_S \hat{U}_C^\dagger \otimes |1\rangle\langle 1|. \quad (S2)$$

Given that the Hamiltonian \hat{H}_C of the generating process satisfies $[\hat{H}_C, [\hat{H}_C, \hat{H}_S]] = [\hat{H}_S, [\hat{H}_C, \hat{H}_S]] = 0$, we have

$$\begin{aligned} \hat{U}_C^\dagger \hat{\mathcal{K}}_S \hat{U}_C &= \int_0^{T_S} e^{i\hat{H}_C T_C} e^{i\hat{H}_S t} \hat{V}_S e^{-i\hat{H}_S t} e^{-i\hat{H}_C T_C} dt \\ &= \int_0^{T_S} e^{i\hat{H}_S t} e^{i\hat{H}_C T_C} e^{-[\hat{H}_C, \hat{H}_S] T_C t} \hat{V}_S e^{-[\hat{H}_S, \hat{H}_C] T_C t} e^{-i\hat{H}_C T_C} e^{-i\hat{H}_S t} dt. \end{aligned}$$

By taking the partial derivative with respect to g on both sides of the equation $[\hat{H}_S, [\hat{H}_C, \hat{H}_S]] = 0$, we can calculate that

$$[\hat{V}_S, [\hat{H}_C, \hat{H}_S]] + [\hat{H}_S, [\hat{H}_C, \hat{V}_S]] = 0.$$

Given that the Hamiltonian \hat{H}_C satisfies $[\hat{H}_C, \hat{V}_S] = i$ in our scheme, we can derive that

$$[\hat{V}_S, [\hat{H}_C, \hat{H}_S]] = 0,$$

which implies that the operator \hat{V}_S commutes with the commutator $[\hat{H}_C, \hat{H}_S]$. Therefore, we can calculate that

$$\hat{U}_C^\dagger \hat{\mathcal{K}}_S \hat{U}_C = \int_0^{T_S} e^{i\hat{H}_S t} e^{i\hat{H}_C T_C} \hat{V}_S e^{-i\hat{H}_C T_C} e^{-i\hat{H}_S t} dt. \quad (S3)$$

Given that $[\hat{H}_C, \hat{V}_S] = i$, we have

$$e^{i\hat{H}_C T_C} \hat{V}_S e^{-i\hat{H}_C T_C} = \hat{V}_S - T_C.$$

Substituting it into Eq. (S3), we can derive that

$$\hat{U}_C^\dagger \hat{\mathcal{K}}_S \hat{U}_C = \hat{\mathcal{K}}_S - T_C T_S. \quad (S4)$$

Similarly, we can derive that

$$\hat{U}_C \hat{\mathcal{K}}_S \hat{U}_C^\dagger = \hat{\mathcal{K}}_S + T_C T_S. \quad (S5)$$

Substituting Eq. (S4) and Eq. (S5) into Eq. (S2), we obtain the expression for $\hat{\mathcal{K}}_I$ as shown in Eq. (3) of the main text. We denote the initial state of the joint system of the probe and ancilla as $\hat{\rho}_{SA} = \hat{\rho}_S \otimes \hat{\rho}_A = \sum_i p_i |\Psi_i\rangle\langle\Psi_i| \otimes |\phi\rangle\langle\phi| = \sum_i p_i |\Psi_i\rangle\langle\Psi_i|$, where $|\Psi_i\rangle = |\psi_i\rangle \otimes |\phi\rangle$, then the average uncertainty of the initial joint state $\hat{\rho}_{SA}$ with respect to the canonical momentum operator $\hat{\mathcal{K}}_I$ can be calculated as

$$\begin{aligned} \Delta \bar{\mathcal{K}}_I^2 &= \sum_i p_i \left(\langle \Psi_i | \hat{\mathcal{K}}_I^2 | \Psi_i \rangle - \langle \Psi_i | \hat{\mathcal{K}}_I | \Psi_i \rangle^2 \right) \\ &= \sum_i p_i \left[\langle \psi_i | \hat{\mathcal{K}}_S^2 | \psi_i \rangle + T_C^2 T_S^2 - 2T_C T_S \langle \psi_i | \hat{\mathcal{K}}_S | \psi_i \rangle \langle \phi | \hat{\sigma}_z | \phi \rangle - \left(\langle \psi_i | \hat{\mathcal{K}}_S | \psi_i \rangle - T_C T_S \langle \phi | \hat{\sigma}_z | \phi \rangle \right)^2 \right] \\ &= \sum_i p_i \left(\langle \psi_i | \hat{\mathcal{K}}_S^2 | \psi_i \rangle - \langle \psi_i | \hat{\mathcal{K}}_S | \psi_i \rangle^2 \right) + T_C^2 T_S^2 - T_C^2 T_S^2 \langle \phi | \hat{\sigma}_z | \phi \rangle^2, \end{aligned}$$

where $\hat{\sigma}_z = |0\rangle\langle 0| - |1\rangle\langle 1|$ is the Pauli operator of the ancilla, thus $\langle\phi|\hat{\sigma}_z|\phi\rangle^2 \leq 1$. Given that

$$\sum_i p_i \left(\langle\psi_i|\hat{\mathcal{K}}_S^2|\psi_i\rangle - \langle\psi_i|\hat{\mathcal{K}}_S|\psi_i\rangle^2 \right) = \Delta\bar{\mathcal{K}}_S^2 \leq \Delta\mathcal{V}_S^2 T_S^2,$$

we can derive

$$\Delta\bar{\mathcal{K}}_I^2 \leq \Delta\mathcal{V}_S^2 T_S^2 + T_C^2 T_S^2. \quad (\text{S6})$$

By assigning $T_C = T_S = T$ and substituting Eq. (S6) into Eq. (1) while replacing $\Delta\bar{\mathcal{K}}_S$ by $\Delta\bar{\mathcal{K}}_I$, we can ultimately derive the precision limit as shown in Eq. (4).

Next, we sequentially apply the parameterizing process $\hat{U}_S(g)$ N times within the standard quantum metrological scheme. Consequently, the total sequential evolution can be expressed as $\hat{U}_S^{(N)} = [\hat{U}_S(g)]^N = \exp[-i\hat{H}_S(g)NT_S]$, given that the Hamiltonian $\hat{H}_S(g)$ is time-independent. In this case, the canonical momentum in the Heisenberg picture can be calculated as

$$\hat{\mathcal{K}}_S^{(N)} = i \left[\hat{U}_S^{(N)} \right]^\dagger \left[\partial_g \hat{U}_S^{(N)} \right] = \int_0^{NT_S} e^{i\hat{H}_S t} \hat{V}_S e^{-i\hat{H}_S t} dt.$$

Drawing on the calculation of the upper bound of $\Delta\bar{\mathcal{K}}_S^2$, we can derive

$$\begin{aligned} \left[\Delta\bar{\mathcal{K}}_S^{(N)} \right]^2 &\leq NT_S \int_0^{NT_S} \sum_i p_i \left(\langle\psi_i|e^{i\hat{H}_S t} \hat{V}_S^2 e^{-i\hat{H}_S t}|\psi_i\rangle - \langle\psi_i|e^{i\hat{H}_S t} \hat{V}_S e^{-i\hat{H}_S t}|\psi_i\rangle^2 \right) dt \\ &= NT_S \int_0^{NT_S} \Delta\bar{V}_S^2|_{\hat{\rho}_t} dt. \end{aligned}$$

where $\hat{\rho}_t = \sum_i p_i e^{-i\hat{H}_S t} |\psi_i\rangle\langle\psi_i| e^{i\hat{H}_S t}$. Given that the average uncertainty of the operator \hat{V}_S is bounded by a maximum value of $\Delta\mathcal{V}_S$, we can finally obtain

$$\left[\Delta\bar{\mathcal{K}}_S^{(N)} \right]^2 \leq NT_S \int_0^{NT_S} \Delta\mathcal{V}_S^2 dt = \Delta\mathcal{V}_S^2 N^2 T_S^2. \quad (\text{S7})$$

By normalizing $T_S = 1$ and substituting Eq. (S7) into Eq. (1) while replacing $\Delta\bar{\mathcal{K}}_S$ by $\Delta\bar{\mathcal{K}}_S^{(N)}$, we can ultimately derive the precision limit as shown in Eq. (5).

Subsequently, we sequentially apply the evolution \hat{U}_{IS} , which comprises an ITD generating process \hat{U}_I prior to the parameterizing process $\hat{U}_S(g)$, in our quantum metrological scheme. Consequently, the total sequential evolution of the joint system of the probe and ancilla can be expressed as $\hat{U}_{IS}^{(N)} = (\hat{U}_S \hat{U}_C)^N \otimes |0\rangle\langle 0| + (\hat{U}_S \hat{U}_C^\dagger)^N \otimes |1\rangle\langle 1|$. In this case, the canonical momentum operator of the joint system (in the Heisenberg picture) can be derived as

$$\begin{aligned} \hat{\mathcal{K}}_I^{(N)} &= i \left[\hat{U}_{IS}^{(N)} \right]^\dagger \left[\partial_g \hat{U}_{IS}^{(N)} \right] \\ &= i \left(\hat{U}_C^\dagger \hat{U}_S^\dagger \right)^N \sum_{i=0}^{N-1} \left(\hat{U}_S \hat{U}_C \right)^{N-1-i} \left(\partial_g \hat{U}_S \right) \hat{U}_C \left(\hat{U}_S \hat{U}_C \right)^i \otimes |0\rangle\langle 0| \\ &\quad + i \left(\hat{U}_C \hat{U}_S^\dagger \right)^N \sum_{i=0}^{N-1} \left(\hat{U}_S \hat{U}_C^\dagger \right)^{N-1-i} \left(\partial_g \hat{U}_S \right) \hat{U}_C^\dagger \left(\hat{U}_S \hat{U}_C^\dagger \right)^i \otimes |1\rangle\langle 1| \\ &= \sum_{i=0}^{N-1} \left(\hat{U}_C^\dagger \hat{U}_S^\dagger \right)^i \hat{U}_C^\dagger \hat{\mathcal{K}}_S \hat{U}_C \left(\hat{U}_S \hat{U}_C \right)^i \otimes |0\rangle\langle 0| + \sum_{i=0}^{N-1} \left(\hat{U}_C \hat{U}_S^\dagger \right)^i \hat{U}_C \hat{\mathcal{K}}_S \hat{U}_C^\dagger \left(\hat{U}_S \hat{U}_C^\dagger \right)^i \otimes |1\rangle\langle 1|. \end{aligned}$$

Given that the Hamiltonian \hat{H}_C of the generating process satisfies $[\hat{H}_C, [\hat{H}_C, \hat{H}_S]] = [\hat{H}_S, [\hat{H}_C, \hat{H}_S]] = 0$, we have

$$\hat{U}_C^\dagger \hat{U}_S^\dagger = e^{-[\hat{H}_C, \hat{H}_S]T_C T_S} \hat{U}_S^\dagger \hat{U}_C^\dagger, \quad \hat{U}_S \hat{U}_C = e^{-[\hat{H}_S, \hat{H}_C]T_C T_S} \hat{U}_C \hat{U}_S.$$

and

$$\hat{U}_C \hat{U}_S^\dagger = e^{[\hat{H}_C, \hat{H}_S]T_C T_S} \hat{U}_S^\dagger \hat{U}_C, \quad \hat{U}_S \hat{U}_C^\dagger = e^{[\hat{H}_S, \hat{H}_C]T_C T_S} \hat{U}_C^\dagger \hat{U}_S.$$

Since the commutator $[\hat{H}_C, \hat{H}_S]$ commutes with the operators \hat{H}_C , \hat{H}_S , and \hat{V}_S , it also commutes with the momentum operator $\hat{\mathcal{K}}_S = \int_0^{T_S} \hat{U}_S^\dagger(0 \rightarrow t) [\partial_g \hat{H}_S(g)] \hat{U}_S(0 \rightarrow t) dt$. Therefore, we can further derive $\hat{\mathcal{K}}_I^{(N)}$ as

$$\begin{aligned}\hat{\mathcal{K}}_I^{(N)} &= \sum_{i=0}^{N-1} \left(\hat{U}_S^\dagger \right)^i \left(\hat{U}_C^\dagger \right)^{i+1} \hat{\mathcal{K}}_S \left(\hat{U}_C \right)^{i+1} \left(\hat{U}_S \right)^i \otimes |0\rangle\langle 0| \\ &\quad + \sum_{i=0}^{N-1} \left(\hat{U}_S^\dagger \right)^i \left(\hat{U}_C \right)^{i+1} \hat{\mathcal{K}}_S \left(\hat{U}_C^\dagger \right)^{i+1} \left(\hat{U}_S \right)^i \otimes |1\rangle\langle 1|.\end{aligned}$$

Combining with Eq. (S4) and Eq. (S5), we can calculate

$$\begin{aligned}\hat{\mathcal{K}}_I^{(N)} &= \sum_{i=0}^{N-1} \left(\hat{U}_S^\dagger \right)^i \hat{\mathcal{K}}_S \left(\hat{U}_S \right)^i \otimes \hat{\mathbb{I}} - \sum_{i=1}^N i T_C T_S \otimes \hat{\sigma}_z \\ &= i \sum_{i=0}^{N-1} \left(\hat{U}_S^\dagger \right)^{i+1} \left(\partial_g \hat{U}_S \right) \left(\hat{U}_S \right)^i \otimes \hat{\mathbb{I}} - \frac{N^2 + N}{2} T_C T_S \otimes \hat{\sigma}_z \\ &= i \left(\hat{U}_S^\dagger \right)^N \sum_{i=0}^{N-1} \left(\hat{U}_S \right)^{N-i-1} \left(\partial_g \hat{U}_S \right) \left(\hat{U}_S \right)^i \otimes \hat{\mathbb{I}} - \frac{N^2 + N}{2} T_C T_S \otimes \hat{\sigma}_z \\ &= i \left[\hat{U}_S^{(N)} \right]^\dagger \left[\partial_g \hat{U}_S^{(N)} \right] \otimes \hat{\mathbb{I}} - \frac{N^2 + N}{2} T_C T_S \otimes \hat{\sigma}_z \\ &= \hat{\mathcal{K}}_S^{(N)} \otimes \hat{\mathbb{I}} - \frac{N^2 + N}{2} T_C T_S \otimes \hat{\sigma}_z,\end{aligned}$$

which is exactly the expression as shown in Eq. (S6). Furthermore, we can calculate its uncertainty of the initial joint state $\hat{\rho}_{SA} = \sum_i p_i |\Psi_i\rangle\langle\Psi_i|$ as

$$\begin{aligned}\left[\Delta \bar{\mathcal{K}}_I^{(N)} \right]^2 &= \sum_i p_i \left(\langle \Psi_i | [\hat{\mathcal{K}}_I^{(N)}]^2 | \Psi_i \rangle - \langle \Psi_i | \hat{\mathcal{K}}_I^{(N)} | \Psi_i \rangle^2 \right) \\ &= \sum_i p_i \left(\langle \psi_i | [\hat{\mathcal{K}}_S^{(N)}]^2 | \psi_i \rangle - \langle \psi_i | \hat{\mathcal{K}}_S^{(N)} | \psi_i \rangle^2 \right) + \frac{(N^2 + N)^2}{4} T_C^2 T_S^2 (1 - \langle \phi | \hat{\sigma}_z | \phi \rangle^2).\end{aligned}$$

Combining with Eq. (S7), we can finally obtain

$$\begin{aligned}\left[\Delta \bar{\mathcal{K}}_I^{(N)} \right]^2 &\leq \left[\Delta \bar{\mathcal{K}}_S^{(N)} \right]^2 + \frac{(N^2 + N)^2}{4} T_C^2 T_S^2 \\ &\leq \Delta \mathcal{V}_S^2 N^2 T_S^2 + \frac{(N^2 + N)^2}{4} T_C^2 T_S^2.\end{aligned}\tag{S8}$$

By normalizing $T_C = T_S = 1$ and substituting Eq. (S8) into Eq. (1) while replacing $\Delta \bar{\mathcal{K}}_S$ by $\Delta \bar{\mathcal{K}}_I^{(N)}$, we can ultimately derive the precision limit as shown in Eq. (7).

Supplementary Note 2: Average uncertainty of final probe state with respect to \hat{V}_S

In the standard quantum metrological scheme with a parameterizing process $\hat{U}_S(g)$, the average uncertainty of the final probe state $\hat{\rho}_f = \sum_i p_i \hat{U}_S |\psi_i\rangle\langle\psi_i| \hat{U}_S^\dagger$ with respect to operator \hat{V}_S can be expressed as

$$\Delta \bar{V}_S^2|_{\hat{\rho}_f} = \sum_i p_i \left(\langle \psi_i | \hat{U}_S^\dagger \hat{V}_S^2 \hat{U}_S | \psi_i \rangle - \langle \psi_i | \hat{U}_S^\dagger \hat{V}_S \hat{U}_S | \psi_i \rangle^2 \right),\tag{S9}$$

while the average uncertainty of the final probe state $\hat{\rho}_f^{(N)} = \sum_i p_i \hat{U}_S^{(N)} |\psi_i\rangle\langle\psi_i| (\hat{U}_S^{(N)})^\dagger$ when applying the parameterizing process N times can be expressed as

$$\begin{aligned}\Delta \bar{V}_S^2|_{\hat{\rho}_f^{(N)}} &= \sum_i p_i \left[\langle \psi_i | \left(\hat{U}_S^{(N)} \right)^\dagger \hat{V}_S^2 \hat{U}_S^{(N)} | \psi_i \rangle - \langle \psi_i | \left(\hat{U}_S^{(N)} \right)^\dagger \hat{V}_S \hat{U}_S^{(N)} | \psi_i \rangle^2 \right] \\ &= \sum_i p_i \left[\langle \psi_i | \left(\hat{U}_S^\dagger \right)^N \hat{V}_S^2 \left(\hat{U}_S \right)^N | \psi_i \rangle - \langle \psi_i | \left(\hat{U}_S^\dagger \right)^N \hat{V}_S \left(\hat{U}_S \right)^N | \psi_i \rangle^2 \right]\end{aligned}\tag{S10}$$

In our scheme, the initial state of the joint system of the probe and ancilla is denoted as $\hat{\rho}_{SA} = \hat{\rho}_S \otimes \hat{\rho}_A = \sum_i p_i |\psi_i\rangle\langle\psi_i| \otimes |\phi\rangle\langle\phi| = \sum_i p_i |\Psi_i\rangle\langle\Psi_i|$, where $|\Psi_i\rangle = |\psi_i\rangle \otimes |\phi\rangle$ and the initial ancilla state can be expressed as $|\phi\rangle = \alpha|0\rangle + \beta|1\rangle$ with $|\alpha|^2 + |\beta|^2 = 1$. By going through a single-shot evolution \hat{U}_{IS} , which comprises an ITD generating process and a parameterizing process, the final state of the joint system is denoted as $\hat{U}_{IS}\hat{\rho}_{SA}\hat{U}_{IS}^\dagger = \sum_i p_i \hat{U}_{IS}|\Psi_i\rangle\langle\Psi_i|\hat{U}_{IS}^\dagger$. Then the final probe state in our scheme can be obtained as

$$\hat{\rho}'_f = \text{Tr}_A (\hat{U}_{IS}\hat{\rho}_{SA}\hat{U}_{IS}^\dagger) = \sum_i p_i |\alpha|^2 \hat{U}_S \hat{U}_C |\psi_i\rangle\langle\psi_i| \hat{U}_C^\dagger \hat{U}_S^\dagger + \sum_i p_i |\beta|^2 \hat{U}_S \hat{U}_C^\dagger |\psi_i\rangle\langle\psi_i| \hat{U}_C \hat{U}_S^\dagger.$$

In this case, the average uncertainty of the final probe state $\hat{\rho}'_f$ with respect to the operator \hat{V}_S can be calculated as

$$\begin{aligned} \Delta\bar{V}_S^2|_{\hat{\rho}'_f} &= \sum_i p_i |\alpha|^2 \left(\langle\psi_i|\hat{U}_C^\dagger \hat{U}_S^\dagger \hat{V}_S^2 \hat{U}_S \hat{U}_C |\psi_i\rangle - \langle\psi_i|\hat{U}_C^\dagger \hat{U}_S^\dagger \hat{V}_S \hat{U}_S \hat{U}_C |\psi_i\rangle^2 \right) \\ &\quad + \sum_i p_i |\beta|^2 \left(\langle\psi_i|\hat{U}_C \hat{U}_S^\dagger \hat{V}_S^2 \hat{U}_S \hat{U}_C^\dagger |\psi_i\rangle - \langle\psi_i|\hat{U}_C \hat{U}_S^\dagger \hat{V}_S \hat{U}_S \hat{U}_C^\dagger |\psi_i\rangle^2 \right). \end{aligned}$$

Given that the Hamiltonian \hat{H}_C of the generating process satisfies $[\hat{H}_C, [\hat{H}_C, \hat{H}_S]] = [\hat{H}_S, [\hat{H}_C, \hat{H}_S]] = 0$ and the commutator $[\hat{H}_C, \hat{H}_S]$ commutes with the operators \hat{H}_C , \hat{H}_S , and \hat{V}_S , we can further calculate

$$\begin{aligned} \Delta\bar{V}_S^2|_{\hat{\rho}'_f} &= \sum_i p_i |\alpha|^2 \left[\langle\psi_i|\hat{U}_S^\dagger (\hat{V}_S - T_C)^2 \hat{U}_S |\psi_i\rangle - \langle\psi_i|\hat{U}_S^\dagger (\hat{V}_S - T_C) \hat{U}_S |\psi_i\rangle^2 \right] \\ &\quad + \sum_i p_i |\beta|^2 \left[\langle\psi_i|\hat{U}_S^\dagger (\hat{V}_S + T_C)^2 \hat{U}_S |\psi_i\rangle - \langle\psi_i|\hat{U}_S^\dagger (\hat{V}_S + T_C) \hat{U}_S |\psi_i\rangle^2 \right] \\ &= \sum_i p_i (|\alpha|^2 + |\beta|^2) \left(\langle\psi_i|\hat{U}_S^\dagger \hat{V}_S^2 \hat{U}_S |\psi_i\rangle - \langle\psi_i|\hat{U}_S^\dagger \hat{V}_S \hat{U}_S |\psi_i\rangle^2 \right) \\ &= \sum_i p_i \left(\langle\psi_i|\hat{U}_S^\dagger \hat{V}_S^2 \hat{U}_S |\psi_i\rangle - \langle\psi_i|\hat{U}_S^\dagger \hat{V}_S \hat{U}_S |\psi_i\rangle^2 \right), \end{aligned}$$

which equals $\Delta\bar{V}_S^2|_{\hat{\rho}_f}$ in Eq. (S9).

Subsequently, when applying the evolution \hat{U}_{IS} in our scheme N times, the final probe state can be obtained as

$$\begin{aligned} \hat{\rho}'_f^{(N)} &= \text{Tr}_A \left[\left(\hat{U}_{IS} \right)^N \hat{\rho}_{SA} \left(\hat{U}_{IS}^\dagger \right)^N \right] \\ &= \sum_i p_i |\alpha|^2 \left(\hat{U}_S \hat{U}_C \right)^N |\psi_i\rangle\langle\psi_i| \left(\hat{U}_C^\dagger \hat{U}_S^\dagger \right)^N + \sum_i p_i |\beta|^2 \left(\hat{U}_S \hat{U}_C^\dagger \right)^N |\psi_i\rangle\langle\psi_i| \left(\hat{U}_C \hat{U}_S^\dagger \right)^N. \end{aligned}$$

Then its average uncertainty with respect to the operator \hat{V}_S can be calculated as

$$\begin{aligned} \Delta\bar{V}_S^2|_{\hat{\rho}'_f^{(N)}} &= \sum_i p_i |\alpha|^2 \left[\langle\psi_i| \left(\hat{U}_C^\dagger \hat{U}_S^\dagger \right)^N \hat{V}_S^2 \left(\hat{U}_S \hat{U}_C \right)^N |\psi_i\rangle - \langle\psi_i| \left(\hat{U}_C^\dagger \hat{U}_S^\dagger \right)^N \hat{V}_S \left(\hat{U}_S \hat{U}_C \right)^N |\psi_i\rangle^2 \right] \\ &\quad + \sum_i p_i |\beta|^2 \left[\langle\psi_i| \left(\hat{U}_C \hat{U}_S^\dagger \right)^N \hat{V}_S^2 \left(\hat{U}_S \hat{U}_C^\dagger \right)^N |\psi_i\rangle - \langle\psi_i| \left(\hat{U}_C \hat{U}_S^\dagger \right)^N \hat{V}_S \left(\hat{U}_S \hat{U}_C^\dagger \right)^N |\psi_i\rangle^2 \right] \\ &= \sum_i p_i |\alpha|^2 \left[\langle\psi_i| \left(\hat{U}_S^\dagger \right)^N (\hat{V}_S - NT_C)^2 \left(\hat{U}_S \right)^N |\psi_i\rangle - \langle\psi_i| \left(\hat{U}_S^\dagger \right)^N (\hat{V}_S - NT_C) \left(\hat{U}_S \right)^N |\psi_i\rangle^2 \right] \\ &\quad + \sum_i p_i |\beta|^2 \left[\langle\psi_i| \left(\hat{U}_S^\dagger \right)^N (\hat{V}_S + NT_C)^2 \left(\hat{U}_S \right)^N |\psi_i\rangle - \langle\psi_i| \left(\hat{U}_S^\dagger \right)^N (\hat{V}_S + NT_C) \left(\hat{U}_S \right)^N |\psi_i\rangle^2 \right] \\ &= \sum_i p_i (|\alpha|^2 + |\beta|^2) \left[\langle\psi_i| \left(\hat{U}_S^\dagger \right)^N \hat{V}_S^2 \left(\hat{U}_S \right)^N |\psi_i\rangle - \langle\psi_i| \left(\hat{U}_S^\dagger \right)^N \hat{V}_S \left(\hat{U}_S \right)^N |\psi_i\rangle^2 \right] \\ &= \sum_i p_i \left[\langle\psi_i| \left(\hat{U}_S^\dagger \right)^N \hat{V}_S^2 \left(\hat{U}_S \right)^N |\psi_i\rangle - \langle\psi_i| \left(\hat{U}_S^\dagger \right)^N \hat{V}_S \left(\hat{U}_S \right)^N |\psi_i\rangle^2 \right], \end{aligned}$$

which equals $\Delta\bar{V}_S^2|_{\hat{\rho}_f^{(N)}}$ in Eq. (S10).

Consequently, our scheme strictly complies with the average uncertainty constraint with respect to the operator \hat{V}_S throughout the metrological process. Notably, the ITD generating process we utilized does not incur additional resource costs in the probe state compared to the standard quantum metrological scheme.

Supplementary Note 3: Calculating experimental precision and RMSE

In this section, we utilize the classical Fisher information (CFI) to determine the theoretical precision limits of our experimental setup, as illustrated in Eq. (11) and Eq. (14) of the main text. Subsequently, we present the optimal estimator for the unknown parameter g in our experiments, along with the methodology for calculating their root-mean-square error (RMSE).

First, based on the classical estimation theory, the CFI for the unknown parameter g with respect to the measurement probabilities $\{P_i | \sum_i P_i = 1\}$ can be calculated by

$$F(g) = \sum_i \frac{1}{P_i} \left(\frac{\partial P_i}{\partial g} \right)^2. \quad (\text{S11})$$

Substituting P_+ and P_- from Eq. (10) into Eq. (S11), we can calculate the CFI for the parameter g with respect to various time lengths T of a single-shot evolution, which comprises a ITD generating process and a parameterizing process, in our experiments as

$$F(g) = T^4 \frac{4 \cos^2(2gT^2)}{1 - \sin^2(2gT^2)} = 4T^4.$$

Then drawing on the classical Cramér-Rao bound theory, the precision limit of estimating the parameter g in the experiments can be obtained as

$$\delta g_{\text{exp}} \geq \frac{1}{\sqrt{\nu F(g)}} = \frac{1}{2\sqrt{\nu T^2}},$$

where ν is the number of measured photons.

Next, by substituting $P_+^{(N)}$ and $P_-^{(N)}$ from Eq. (13) into Eq. (S11), we can calculate the CFI for the parameter g (which equals the rotation angle α in this setting) with respect to various numbers N of sequential evolutions in our experiments as

$$F(\alpha) = (N^2 + N)^2 \frac{\cos^2[(N^2 + N)^2 \alpha]}{1 - \sin^2[(N^2 + N)^2 \alpha]} = (N^2 + N)^2.$$

Then, drawing on the classical Cramér-Rao bound theory, the precision limit of estimating the parameter g in the experiments can be obtained as

$$\delta g_{\text{exp}}^{(N)} = \delta \alpha \geq \frac{1}{\sqrt{\nu F(\alpha)}} = \frac{1}{\sqrt{\nu(N^2 + N)}}.$$

In the experiments, the estimated value \tilde{g} of the parameter g can be obtained from the detected photons number $\tilde{\nu}_+$ under the projection $\hat{\Pi}_+$ and the detected photons number $\tilde{\nu}_-$ under the projection $\hat{\Pi}_-$. To derive the expression of the estimator \tilde{g} from the measurement results $\tilde{\nu}_+$ and $\tilde{\nu}_-$, we first calculate the log-likelihood function for the unknown parameter g as

$$\begin{aligned} \ell(g | \{\tilde{\nu}_+, \tilde{\nu}_-\}) &= \ln \left(\mathcal{P}_0 \prod_{i=+,-} P_i^{\tilde{\nu}_i} \right) \\ &= \ln \mathcal{P}_0 + \sum_{i=+,-} \tilde{\nu}_i P_i, \end{aligned}$$

where

$$\ln \mathcal{P}_0 = \frac{(\sum_i \tilde{\nu}_i)!}{\prod_i \tilde{\nu}_i!},$$

accounts for all possible permutations. Then, by solving the likelihood equation

$$\frac{\partial}{\partial g} \ell(g | \{\tilde{\nu}_+, \tilde{\nu}_-\}) = 0,$$

we can obtain the estimated value \tilde{g} from measured data $\tilde{\nu}_+$ and $\tilde{\nu}_-$. The RMSE of estimating the parameter g in the experiments can be calculated from

$$\text{RMSE}(g) = \sqrt{\frac{1}{M} \sum_i (\tilde{g}^{(i)} - g_0)^2},$$

where g_0 is the true value of parameter g we set in the experiments, M is the number of the measurements repeated (which is 30 in our experiments), and $\tilde{g}^{(i)}$ is the estimated value of i -th measurement.

Furthermore, by substituting P_+ and P_- from Eq. (10) into the likelihood equation, we can calculate the estimator of the parameter g with respect to various time lengths T of a single-shot evolution, which comprises a ITD generating process and a parameterizing process, in our experiments as

$$\tilde{g}_{\text{exp}} = \frac{1}{2T^2} \arcsin \left(\frac{\tilde{\nu}_+ - \tilde{\nu}_-}{\tilde{\nu}_+ + \tilde{\nu}_-} \right).$$

Next, by substituting $P_+^{(N)}$ and $P_-^{(N)}$ from Eq. (13) into the likelihood equation, we can calculate the estimator of the parameter g (which equals the rotation angle α in this setting) with respect to various numbers N of sequential evolutions in our experiments as

$$\tilde{g}_{\text{exp}}^{(N)} = \tilde{\alpha}_{\text{exp}} = \frac{1}{N^2 + N} \arcsin \left(\frac{\tilde{\nu}_+ - \tilde{\nu}_-}{\tilde{\nu}_+ + \tilde{\nu}_-} \right).$$

Algorithm 1: Calculation of coincidence counts

```

/* Assume that SPD A detects the herald photons and SPD B detects the signal photons. For a
single-photon pair, the herald photon should be detected by SPD A before the signal photon is
detected by SPD B. */
```

Input: Timestamps from SPD A and SPD B: $\mathcal{T}_A = \{t_1^{(A)}, t_2^{(A)}, \dots, t_m^{(A)}\}$, $\mathcal{T}_B = \{t_1^{(B)}, t_2^{(B)}, \dots, t_n^{(B)}\}$.

Output: Coincidence counts $\mathcal{C} = \{c_1, c_2, \dots, c_k\}$ between SPD A and SPD B; Corresponding delay times $T = \{t_1, t_2, \dots, t_k\}$ of signal photons.

Initialize T ; /* The step size is set to 5ps and the span ranges from 1ns to 50ns in our experiments. */

Initialize \mathcal{C} ; /* The values of coincidence counts are all set to 0. */

Define $\mathcal{T}_I = \{t_1^{(I)}, t_2^{(I)}, \dots, t_n^{(I)}\}$; /* \mathcal{T}_I is the set of the time intervals between every detected
single-photon pair. */

Set w ; /* w is the gate width for coincidence counting, which is set to 2ns in our experiments. */

/* Search the time intervals between every detected single-photon pair. */

for $i \leftarrow 1$ to n do

for $j \leftarrow 1$ to m do

if $t_i^{(B)} - t_j^{(A)} > 0$ then

$t_i^{(I)} \leftarrow t_i^{(B)} - t_j^{(A)}$

else

| Break to the outer for loop

end

end

end

/* Calculate the coincidence counts with different delay times in T */

for $i \leftarrow 1$ to k do

for $j \leftarrow 1$ to n do

if $t_j^{(I)} > t_i - w/2$ and $t_j^{(I)} < t_i + w/2$ then

$c_i = c_i + 1$

end

end

end

Supplementary Note 4: Algorithm of calculating coincidence counts

In our experiments, we recorded the timestamps of the detected photons for each single-photon detector (SPD) using the Moku:Pro device provided by Liquid Instruments, which offers a time jitter of less than 20 ps. We supplemented the original timestamp data detected by the three SPDs with eight individual files. These files correspond to an evolution time length T of 1, 2, 3, and 4 for a single-shot evolution ($N = 1$), and an iteration numbers N of 1, 2, 3, and 4 for a normalized time length ($T = 1$), respectively. Each file contains three columns of timestamp data, corresponding to the timestamps of pulse signals outputted by SPD 1, SPD 2, and SPD 3, respectively. Subsequently, we calculated the coincidence counts between SPD 2 and SPD 1, as well as between SPD 3 and SPD 1, using the timestamp data in each file.

In this work, we developed an algorithm for calculating the coincidence counts between the timestamp data of two different SPDs. This algorithm searches the time intervals between every detected single-photon pair and then determines the coincidence counts with various delay times of the signal photons. This method offers lower computational complexity and reduced computation time compared to the traditional approach of shifting the timestamps of signal photons to calculate the coincidence counts. The detailed algorithm is presented in Algorithm 1.

Based on this algorithm, we calculated the coincidence counts between SPD 2 and SPD 1, as well as between SPD 3 and SPD 1, with varying delay times of the signal photons. In our calculations, the delay times range from 1 ns to 50 ns, with a step size of 5 ps. Considering the time jitter in SPDs, the gate width for coincidence counting in our calculations is set to 2 ns. Subsequently, the number of detected photons, $\tilde{\nu}_+$, under the projection $\hat{\Pi}_+$ and the number of detected photons, $\tilde{\nu}_-$, under the projection $\hat{\Pi}_-$ can be determined from the peak values of the coincidence counts between SPD 2 and SPD 1, and between SPD 3 and SPD 1, respectively.

In our experiments, we recorded the event timestamps from SPD 1, SPD 2, and SPD 3 over a duration of 30 s for each set of T and N . The data were then divided into 600 groups, with each group representing the timestamps of photon counts within 50 ms. For each set of T and N , we calculated the coincidence counts for these 600 groups between SPD 2 and SPD 1, and between SPD 3 and SPD 1, using a sampling time length of 50 ms.

The results are provided in eight individual files, corresponding to an evolution time length T of 1, 2, 3, and 4 for a single-shot evolution ($N = 1$), and iteration numbers N of 1, 2, 3, and 4 for a normalized time length ($T = 1$). In each file, data labeled as 'Time' represents the delay time axis, data labeled as 'CoinCount1' represents the coincidence counts between SPD 2 and SPD 1 for the 600 groups, and data labeled as 'CoinCount2' represents the coincidence counts between SPD 3 and SPD 1 for the 600 groups.

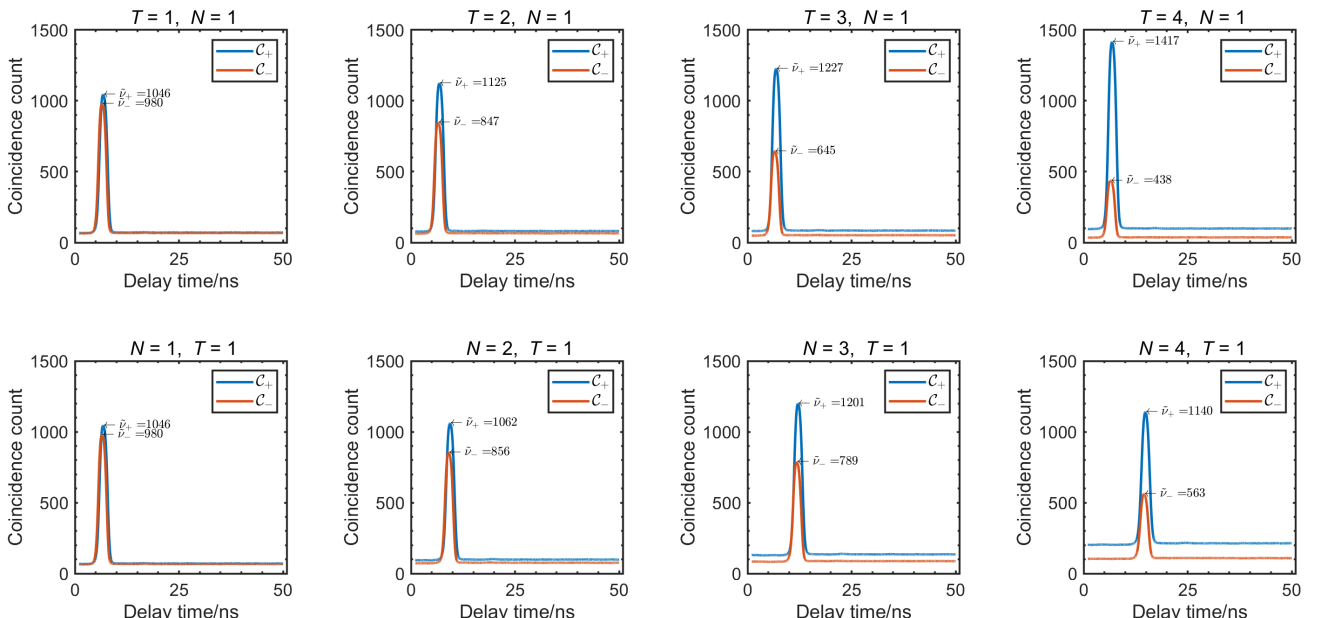


Figure S1. Experimental results of coincidence counts with different evolution time length T of the ITD generating process and the parameterizing process and iteration number N of the identical evolution. The blue curves represent the coincidence counts C_+ between SPD 2 and SPD 1, i.e., the detected results under the projection $\hat{\Pi}_+$, and the orange curves represent the coincidence counts C_- between SPD 3 and SPD 1, i.e., the detected results under the projection $\hat{\Pi}_-$.

As shown in Figure S1, we present the experimental results of coincidence counts between SPD 2 and SPD 1, and between SPD 3 and SPD 1, for various sets of T and N . These results are averaged over the corresponding 600 groups, where the blue curves represent the coincidence counts \mathcal{C}_+ between SPD 2 and SPD 1, and the orange curves represent the coincidence counts \mathcal{C}_- between SPD 3 and SPD 1. The peak values in each curve are marked, which determine the number of detected photons $\tilde{\nu}_+$ under the projection $\hat{\Pi}_+$ and the number of detected photons $\tilde{\nu}_-$ under the projection $\hat{\Pi}_-$ for each set of T and N , respectively.